

Molecular Structure and Solid-state Properties of the Two-dimensional Conducting Mixed-valence Complex $[\text{NBu}_4]_{0.29}[\text{Ni}(\text{dmit})_2]$ and the Neutral $[\text{Ni}(\text{dmit})_2]$ ($\text{H}_2\text{dmit} = 4,5\text{-dimercapto-1,3-dithiole-2-thione}$); † Members of an Electron-transfer Series

Lydie Valade, Jean-Pierre Legros, Michèle Bousseau, and Patrick Cassoux*

Laboratoire de Chimie de Coordination du CNRS, associé à l'Université Paul Sabatier, 205 route de Narbonne, 31 400 Toulouse, France

Mary Garbaskas and Leonard V. Interrante

General Electric R & D Center, P.O. Box 8, Schenectady, New York 12301, U.S.A.

Single crystals of the mixed-valence radical salt $[\text{NBu}_4]_2[\text{Ni}(\text{dmit})_2] \cdot 2\text{CH}_3\text{CN}$ {ignoring the solvent molecules, the formula may be written as $[\text{NBu}_4]_{0.29}[\text{Ni}(\text{dmit})_2]$; $\text{H}_2\text{dmit} = 4,5\text{-dimercapto-1,3-dithiole-2-thione}$ } were obtained by galvanostatic oxidation of $[\text{NBu}_4][\text{Ni}(\text{dmit})_2]$ in acetonitrile. The crystal structure of this compound has been determined at 118 K by X-ray diffraction studies: crystals are triclinic, space group $P1$ or $P\bar{1}$ (assumed), with $Z = 2$ and unit-cell dimensions $a = 13.425(2)$, $b = 22.791(3)$, $c = 24.183(4)$ Å, $\alpha = 108.49(1)$, $\beta = 103.02(1)$, and $\gamma = 89.82(1)^\circ$. The structure was solved by direct methods and refined by least squares to $R = 0.038$ for 7 170 unique, observed, diffractometer data. It consists of thick layers of stacked $\text{Ni}(\text{dmit})_2$ entities parallel to (001), and separated by sheets of $[\text{NBu}_4]^+$ cations and CH_3CN molecules. Strong π interactions within a stack are evidenced by the short stacking distances (3.48–3.57 Å). There is also an extensive interleaving of the $\text{Ni}(\text{dmit})_2$ which involves close $\text{S} \cdots \text{S}$ interstack contacts. As a result, this structural arrangement is nearly two-dimensional. Conductivity measurements, carried out using a four-probe technique, show a high ($\sigma = 1\text{--}10 \Omega^{-1} \text{cm}^{-1}$ at 300 K) thermally activated ($E_a = 0.1\text{--}0.02$ eV) conductivity. Measurements of the conductivity along the b and a axes, using the Montgomery method, show a low anisotropy (σ_b/σ_a ca. 1), consistent with the two-dimensional nature of this compound. The related neutral member of the $[\text{Ni}(\text{dmit})_2]^{n-}$ electron-transfer series ($n = 0$) has been isolated for the first time and its crystal structure determined: crystals are monoclinic, space group $P2_1/a$, with $Z = 2$, $a = 17.108(9)$, $b = 5.302(4)$, $c = 7.720(4)$ Å, and $\beta = 77.09(4)^\circ$. The structure was solved by direct methods and refined by least squares to $R = 0.041$ for 772 unique, observed, diffractometer data. The structure of this semi-conducting compound consists of regular stacks of $\text{Ni}(\text{dmit})_2$ along the [010] direction with short interstack $\text{S} \cdots \text{S}$ distances.

The interest in molecular co-ordination compounds exhibiting unusual solid-state properties, which began with the spectral studies of Yamada and co-workers on Magnus' Green salt¹ and nickel dimethylglyoximate,² was later strongly enhanced by the prospect,³ subsequently realized,⁴ that solid-state interactions could give rise to novel electrical properties. Eventually this work on co-ordination compounds with one-dimensional metal-like characteristics, such as $\text{K}_2[\text{Pt}(\text{CN})_4]\text{Br}_{0.3} \cdot 3\text{H}_2\text{O}$,⁵ merged with the efforts on the one-dimensional 'organic metals' (e.g. $\text{ttf} \cdot \text{tcnq}^\ddagger$ and related π donor-acceptor compounds).⁶ Finally, the hope that such systems could serve as a new source of superconducting materials⁷ was confirmed in studies of the $(\text{tmtsf})_2\text{X}$ radical salts,⁸ resulting in a further intensification of the strong interest in such 'low-dimensional' systems.⁶⁻⁹

Until recently, structural studies of most of the highly conducting molecular systems supported the view of these materials as quasi one-dimensional systems containing clearly defined and largely isolated, parallel stacks of the constituent planar molecules.⁶ However, the low-temperature electronic instability (Peierls transition¹⁰) inherent in such systems usually

results in a metal-to-insulator transition rather than superconductivity on cooling to low temperatures. Recent work on compounds of the $(\text{tmtsf})_2\text{X}$ ^{8,11,12} and $(\text{bedttf})_2\text{X}$ ¹³⁻¹⁶ series has shown that one of the principal requirements for retention of metal-like characteristics and eventual transition to a superconductive state at low temperature is higher-than-one dimensionality, that is strong interchain electronic interactions. We have recently obtained evidence for such 'multi-dimensional' interactions in the new highly conducting $[\text{ttf}][\text{Ni}(\text{dmit})_2]_2$ compound¹⁷ derived from the nickel complex of the dmit^{2-} ligand; $\text{H}_2\text{dmit} = 4,5\text{-dimercapto-1,3-dithiole-2-thione}$.

Steimecke and co-workers¹⁸ were the first to prepare transition-metal complexes of the electron-transfer series $[\text{M}(\text{dmit})_2]^{n-}$ and have determined the structures of $[\text{NBu}_4]_2[\text{Ni}(\text{dmit})_2]$ and $[\text{NBu}_4][\text{Ni}(\text{dmit})_2]$.^{19,20} Preliminary studies of these complexes as a source of conducting compounds have been reported by Papavassiliou²¹ and ourselves.^{17,22} We report here in detail the electro-synthesis, crystal structure, and electrical properties of the two-dimensional conducting mixed-

† Supplementary data available (No. SUP 56145, 14 pp.): thermal parameters, H-atom co-ordinates, remaining bond lengths and angles. See Instructions for Authors, *J. Chem. Soc., Dalton Trans.* 1985, Issue 1, pp. xvii-xix. Structure factors are available from the editorial office. Non-S.I. unit employed: $\text{eV} \approx 1.60 \times 10^{-19}$ J.

‡ Abbreviations used: ttf = tetrathiafulvalene [2-(1',3'-dithiol-2'-ylidene)-1,3-dithiole]; tcnq = tetracyanoquinodimethane; tmtsf = tetramethyltetraselenafulvalene [2-(4',5'-dimethyl-1',3'-diselenol-2'-ylidene)-4,5-dimethyl-1,3-diselenole]; bedttf = bis(ethylenedithio)-tetrathiafulvalene {2-(5',6'-dihydro-1',3'-dithio[4,5-*b*][1,4]dithiin-2'-ylidene)-5,6-dihydro-1,3-dithio[4,5-*b*][1,4]dithiin}.

valence salt $[\text{NBu}_4]_{0.29}[\text{Ni}(\text{dmit})_2]$. Some aspects of this work have appeared in preliminary communications.^{23,24} In order to provide a better structure solution by reducing thermal motion and to resolve questions of possible structural changes occurring on cooling, the crystal structure of this compound has now been redetermined at low temperatures. Also, to assist in the interpretation of possible structure-property relationships within the $[\text{Ni}(\text{dmit})_2]^{2-}$ electron-transfer series, the related neutral member, $[\text{Ni}(\text{dmit})_2]$, has been isolated for the first time and its crystal structure determined.

Experimental

Syntheses.—*The dmit²⁻ ligand.* This very unstable ligand was generated in solution by chemical reduction of carbon disulphide with sodium and stabilized as its $[\text{NBu}_4]_2[\text{Zn}(\text{dmit})_2]$ salt, following a procedure combining those described by Hartke *et al.*²⁵ and Steimecke and co-workers,¹⁸ with some modifications. Typically, sodium (5.9 g) was dissolved, at -5°C and under inert atmosphere, in CS_2 (100 cm^3) and dimethylformamide (dmf, 200 cm^3). After dissolution, two more 5.9-g portions of sodium and 15- cm^3 portions of CS_2 were added slowly. This step-by-step addition process takes 5 h, during which the temperature of -5°C was maintained. Finally, CS_2 (25 cm^3) and dmf (100 cm^3) were added. The solution was treated with methanol (50 cm^3) to destroy unreacted sodium. The remaining CS_2 and the dmf were evaporated under vacuum at a temperature not exceeding 40°C . The residue was dissolved in methanol (240 cm^3) and water (120 cm^3). To this solution were rapidly added $\text{ZnSO}_4 \cdot 7\text{H}_2\text{O}$ (14.4 g) dissolved in aqueous ammonia (200 cm^3) and NBu_4Br (32.2 g) dissolved in water (100 cm^3). A purple crystalline powder precipitated, which was collected by filtration and washed with Pr^iOH and diethyl ether. Recrystallization from acetone-isopropyl alcohol (1:1) yielded 38 g of $[\text{NBu}_4]_2[\text{Zn}(\text{dmit})_2]$. For subsequent reactions, the dmit^{2-} anion was regenerated, according to Steimecke and co-workers,¹⁸ by the action of benzoyl chloride followed by treatment with sodium methoxide.

Alternatively, the dmit^{2-} ligand can be prepared by electrochemical reduction of CS_2 .²⁶⁻²⁸ In that case the dmit^{2-} anion can be stabilized by treatment with methyl iodide,²⁶ but we preferred the reaction with benzoyl chloride. The yields obtained with the electrochemical method are much poorer due to clogging of the frit between the anode and cathode compartments.

The $[\text{NBu}_4]_n[\text{Ni}(\text{dmit})_2]$ complexes ($n = 2$ or 1). These complexes were prepared from the dibenzoyl derivative of dmit following the procedures described by Steimecke and co-workers.¹⁸

Bromine oxidation of $[\text{NBu}_4][\text{Ni}(\text{dmit})_2]$. The salt $[\text{NBu}_4][\text{Ni}(\text{dmit})_2]$ (1 mmol) was dissolved in acetonitrile (100 cm^3). To this solution, cooled to -15°C , was added 1 mmol equiv. of bromine dissolved in acetonitrile (50 cm^3). A black and shiny microcrystalline powder precipitated and was collected by filtration, washed intensively with acetonitrile, and dried under vacuum. This material is very insoluble in common solvents. Elemental analysis (Found: C, 17.3; H, 0.7; Ni, 11.5; S, 70.2. $\text{C}_6\text{NiS}_{10}$ requires C, 15.95; H, 0.00; Ni, 13.0; S, 71.05%) shows that the oxidation process was not complete and that the neutral complex $[\text{Ni}(\text{dmit})_2]$ was not obtained. The compaction powder electrical conductivity is ca. $1 \Omega^{-1} \text{cm}^{-1}$.

Electrosynthesis of $[\text{NBu}_4]_{0.29}[\text{Ni}(\text{dmit})_2]$. Single crystals of this salt were obtained by galvanostatic anodic oxidation of $[\text{NBu}_4][\text{Ni}(\text{dmit})_2]$ ($2 \times 10^{-3} \text{mol dm}^{-3}$) in purified acetonitrile containing NBu_4ClO_4 ($10^{-1} \text{mol dm}^{-3}$) as supporting electrolyte. A nitrogen-flushed U-type cell where the anode and cathode are separated by a medium-porosity frit was used with

platinum electrodes. Cleaning of the electrodes prior to use was carried out by treatment with *aqua regia* followed by successive anodic and cathodic polarization of the electrode which is used as anode in dilute sulphuric acid. The temperature of the cell (10°C) and the current ($I = 1 \mu\text{A}$; current density = ca. 10^{-5}A cm^{-2}) were held constant. The crystals formed on the anode were collected on a glass frit, washed with purified acetonitrile, and vacuum dried. Two kinds were obtained, thin needles (typically $1.5 \times 0.04 \times 0.01 \text{mm}$) and platelets ($0.3 \times 0.3 \times 0.05 \text{mm}$). When platinum wire (diameter 0.1 mm) was used as anode the majority of the crystals were of the needle type. In subsequent experiments, a spherical single-crystal platinum anode, prepared according to Clavilier *et al.*,²⁹ was used and the number and size of the platelet-type crystals increased. Also, decreasing the supporting electrolyte concentration to $2 \times 10^{-3} \text{mol dm}^{-3}$ encourages the formation of larger crystals (up to $3 \times 0.1 \times 0.02 \text{mm}$ for needles and $0.9 \times 0.9 \times 0.3 \text{mm}$ for platelets). Both kinds of crystals were characterized by electron microprobe analysis as having the same formula $[\text{NBu}_4]_{0.29}[\text{Ni}(\text{dmit})_2]$. In the case of platelets, this formula was confirmed by the crystal structure determination {Found: Ni, 11.2; S, 61.3. $[\text{NBu}_4]_2[\text{Ni}(\text{dmit})_2] \cdot 2\text{CH}_3\text{CN}$ requires Ni, 11.05; S, 60.2%}.

The complex $[\text{Ni}(\text{dmit})_2]$. During the course of the synthesis of $[\text{tff}][\text{Ni}(\text{dmit})_2]_2$,¹⁷ by slow interdiffusion of acetonitrile solutions of $[\text{tff}]_3[\text{BF}_4]_2$ and $[\text{NBu}_4][\text{Ni}(\text{dmit})_2]$, we had observed and sorted out a few crystals whose morphology (platelet) was different from that (needle) of the majority species. Moreover, the conductivity of these crystals ($3.5 \times 10^{-3} \Omega^{-1} \text{cm}^{-1}$ at 293 K) was markedly different from the value obtained for $[\text{tff}][\text{Ni}(\text{dmit})_2]_2$ ($300 \Omega^{-1} \text{cm}^{-1}$). These crystals were finally characterized by crystal structure determination as being of the neutral complex $[\text{Ni}(\text{dmit})_2]$.

Conductivity Measurements.—Four-probe conductivity measurements were carried out using a Keithley model 225 current source and a model 616 electrometer. The crystals were glued (GE 7031 varnish) on a fibre and attached in the middle of a printed circuit chip equipped with four gold wires (diameter 0.02 mm) soldered to the connectors of the circuit. Electrical contacts to the crystals were made by using Emerton M8001 gold paint. The mounted crystals were placed in an Oxford Instruments CF 200 continuous-flow cryostat for temperature-dependent measurements. Monitoring of the temperature variations was by use of an Oxford Instruments DTC2 temperature controller driven by a home-made voltage ramp programmer.³⁰ Measurements on up to 12 different (needles and platelets) crystals from different batches were performed and gave consistent results.

Temperature-dependent measurements of the anisotropy in the conductivities by the Montgomery method³¹ were carried out on a platelet-type crystals of $[\text{NBu}_4]_{0.29}[\text{Ni}(\text{dmit})_2]$, using the apparatus described above. The platelet crystals were oriented on an automatic X-ray diffractometer to determine the relationship between the measured conductivities and the crystallographic directions.

Other Physical Measurements.—Elemental analyses were performed at our laboratory and at the Service Central de Microanalyses du CNRS. Electron microprobe analysis were performed on a CAMECA model MS46 camera. I.r. spectra were recorded on a Perkin-Elmer, model 577 spectrophotometer.

Single-crystal X-Ray Data Collection and Structure Refinement.—(a) For $[\text{NBu}_4]_{0.29}[\text{Ni}(\text{dmit})_2]$. *Crystal data.* $[\text{NBu}_4]_2[\text{Ni}(\text{dmit})_2] \cdot 2\text{CH}_3\text{CN}$, $M = 3726.6$, triclinic, space group $P1$ or $P\bar{1}$; at $T = 118 \text{K}$, $a = 13.425(2)$, $b = 22.791(3)$, $c = 24.183(4)$ Å, $\alpha = 108.49(1)^\circ$, $\beta = 103.02(1)^\circ$, $\gamma = 89.82(1)^\circ$, $U = 6818 \text{Å}^3$,

Table 1. Fractional atomic co-ordinates of non-hydrogen atoms of $[\text{NBu}_4]_2[\text{Ni}(\text{dmit})_2] \cdot 2\text{CH}_3\text{CN}$ with estimated standard deviations in parentheses

Atom*	X/a	Y/b	Z/c	Atom*	X/a	Y/b	Z/c
Ni(1)	0	0.5	0.5	C(16)	0.198(1)	0.118 2(6)	0.545 8(6)
S(11)	0.142 2(3)	0.484 1(2)	0.553 5(2)	C(26)	0.139(1)	0.166 5(6)	0.562 5(6)
S(21)	-0.075 6(3)	0.518 1(2)	0.573 2(2)	C(36)	0.232(1)	0.143(6)	0.661 1(6)
S(31)	0.205 7(3)	0.491 8(2)	0.684 0(2)	C(46)	0.066 6(9)	0.116 1(6)	0.295 8(6)
S(41)	0.003 1(3)	0.523 8(2)	0.702 4(2)	C(56)	0.008(1)	0.165 1(6)	0.313 1(6)
S(51)	0.166 6(3)	0.515 8(2)	0.805 6(2)	C(66)	-0.020 2(9)	0.140 9(5)	0.198 7(5)
C(11)	0.117(1)	0.496 4(6)	0.621 4(6)	Ni(8)	0.338 0(1)	0.288 72(8)	0.608 02(8)
S(21)	0.019(1)	0.511 3(6)	0.631 4(6)	S(17)	0.436 7(3)	0.234 4(2)	0.652 7(2)
S(31)	0.124(1)	0.511 4(6)	0.735 5(6)	S(27)	0.303 6(3)	0.346 9(2)	0.689 7(2)
Ni(2)	0.103 5(1)	0.640 08(9)	0.429 25(9)	S(37)	0.508 6(3)	0.248 4(2)	0.784 4(1)
S(12)	0.243 2(3)	0.624 3(2)	0.484 9(2)	S(47)	0.373 7(3)	0.347 7(2)	0.817 2(2)
S(22)	0.024 3(3)	0.659 6(2)	0.501 0(2)	S(57)	0.510 0(3)	0.310 0(2)	0.913 2(2)
S(32)	0.300 1(3)	0.632 7(2)	0.615 4(2)	S(67)	0.368 0(3)	0.229 1(2)	0.525 6(2)
S(42)	0.094 9(3)	0.664 5(2)	0.630 0(2)	S(77)	0.246 2(3)	0.345 2(2)	0.563 8(2)
S(52)	0.253 2(3)	0.656 8(2)	0.734 8(2)	S(87)	0.298 4(3)	0.228 5(2)	0.398 0(2)
S(62)	0.181 6(3)	0.617 5(2)	0.357 4(2)	S(97)	0.184 7(3)	0.338 2(2)	0.433 7(2)
S(72)	-0.035 1(3)	0.657 9(2)	0.374 3(2)	S(107)	0.185 1(3)	0.279 8(2)	0.305 2(2)
S(82)	0.109 3(3)	0.607 4(2)	0.226 6(2)	C(17)	0.435 8(9)	0.269 3(5)	0.725 6(5)
S(92)	-0.089 5(3)	0.650 8(2)	0.243 4(2)	C(27)	0.371 1(9)	0.318 3(5)	0.740 9(5)
S(102)	-0.046 1(3)	0.619 1(2)	0.122 4(2)	C(37)	0.465 2(9)	0.302 5(5)	0.842 8(5)
C(12)	0.215(1)	0.637 6(6)	0.552 4(6)	C(47)	0.303(1)	0.259 5(6)	0.473 5(6)
C(22)	0.117(1)	0.653 8(6)	0.560 3(6)	C(57)	0.247(1)	0.312 3(6)	0.490 4(6)
C(32)	0.215(1)	0.651 7(6)	0.664 0(6)	C(67)	0.222(1)	0.282 9(6)	0.376 3(6)
C(42)	0.091 2(9)	0.623 2(5)	0.298 3(5)	Ni(8)	0.451 3(1)	0.430 19(8)	0.536 38(8)
C(52)	-0.004(1)	0.643 9(6)	0.306 9(6)	S(18)	0.547 3(3)	0.374 2(2)	0.580 1(2)
C(62)	-0.009(1)	0.625 1(6)	0.193 8(6)	S(28)	0.417 8(3)	0.487 9(2)	0.619 3(2)
Ni(3)	0.344 5(1)	0.788 60(8)	0.606 69(8)	S(38)	0.611 9(3)	0.382 2(2)	0.710 8(2)
S(13)	0.482 9(3)	0.767 7(2)	0.660 3(2)	S(48)	0.490 4(3)	0.486 8(2)	0.747 0(2)
S(23)	0.268 8(2)	0.812 4(3)	0.679 8(2)	S(58)	0.610 3(3)	0.436 8(2)	0.839 7(2)
S(33)	0.540 1(3)	0.773 0(2)	0.789 5(2)	S(68)	0.488 4(3)	0.374 5(2)	0.454 0(2)
S(43)	0.346 0(3)	0.820 2(2)	0.810 0(2)	S(78)	0.351 2(3)	0.484 1(2)	0.492 4(2)
S(53)	0.506 7(3)	0.811 5(2)	0.913 0(1)	S(88)	0.409 7(3)	0.372 8(2)	0.325 5(2)
S(63)	0.420 9(3)	0.768 0(2)	0.534 7(2)	S(98)	0.281 2(3)	0.473 7(2)	0.361 6(2)
S(73)	0.204 7(3)	0.806 2(2)	0.552 7(2)	S(108)	0.275 4(3)	0.417 1(2)	0.233 0(2)
S(83)	0.348 2(3)	0.763 9(2)	0.406 1(2)	C(18)	0.546(1)	0.408 5(6)	0.653 2(6)
S(93)	0.144 7(3)	0.798 6(2)	0.422 5(2)	C(28)	0.489(1)	0.458 1(6)	0.671 6(6)
S(103)	0.191 5(3)	0.774 9(2)	0.302 8(2)	C(38)	0.572(1)	0.437 1(6)	0.770 1(6)
C(13)	0.454 9(9)	0.780 9(5)	0.727 8(5)	C(48)	0.414(1)	0.402 4(6)	0.401 2(6)
C(23)	0.361 6(9)	0.801 9(5)	0.736 8(5)	C(58)	0.353(1)	0.450 3(6)	0.419 3(6)
C(33)	0.466 9(9)	0.801 4(5)	0.841 1(5)	C(68)	0.324(1)	0.419 1(6)	0.303 8(6)
C(43)	0.330(1)	0.776 8(6)	0.478 1(6)	N(1)	0.282 2(8)	0.870 6(4)	0.052 4(5)
C(53)	0.233(1)	0.793 1(6)	0.485 7(6)	C(101)	0.247(1)	0.802 7(6)	0.035 2(6)
C(63)	0.225(1)	0.778 0(6)	0.372 9(6)	C(102)	0.247(1)	0.780 3(6)	0.089 0(6)
Ni(4)	0.452 7(1)	0.929 31(8)	0.540 26(8)	C(103)	0.202(1)	0.712 4(6)	0.064 5(6)
S(14)	0.591 8(3)	0.909 7(2)	0.593 5(2)	C(104)	0.207(1)	0.687 8(6)	0.117 0(6)
S(24)	0.377 0(3)	0.950 9(2)	0.613 3(2)	C(105)	0.387(1)	0.886 7(6)	0.098 3(6)
S(34)	0.650 2(3)	0.914 7(2)	0.723 8(2)	C(106)	0.474(1)	0.851 9(6)	0.074 7(6)
S(44)	0.452 3(3)	0.956 7(2)	0.742 7(2)	C(107)	0.570(1)	0.865 1(6)	0.127 7(6)
S(54)	0.604 7(3)	0.936 8(2)	0.843 5(2)	C(108)	0.662(1)	0.834 7(6)	0.105 8(7)
S(64)	0.526 6(3)	0.909 0(2)	0.466 2(2)	C(109)	0.210(1)	0.914 0(6)	0.082 6(6)
S(74)	0.312 3(3)	0.948 5(2)	0.488 3(2)	C(110)	0.100(1)	0.909 0(6)	0.044 9(6)
S(84)	0.446 3(3)	0.905 1(2)	0.337 2(2)	C(111)	0.040(1)	0.959 4(6)	0.082 9(6)
S(94)	0.246 9(3)	0.942 2(2)	0.358 3(2)	C(112)	-0.071(1)	0.958 5(7)	0.048 1(7)
S(104)	0.284 0(3)	0.919 8(2)	0.237 6(2)	C(113)	0.290 2(9)	0.883 2(5)	-0.005 0(6)
C(14)	0.564(1)	0.924 4(6)	0.661 8(6)	C(114)	0.319(1)	0.949 8(6)	0.003 1(6)
C(24)	0.469 1(9)	0.943 1(6)	0.669 9(6)	C(115)	0.335(1)	0.954 7(6)	-0.057 1(6)
C(34)	0.572(1)	0.935 5(6)	0.773 9(6)	C(116)	0.362(1)	1.022 2(6)	-0.051 4(6)
C(44)	0.432(1)	0.916 4(6)	0.409 1(6)	N(2)	0.283 7(8)	0.368 3(4)	0.049 6(5)
C(54)	0.336(1)	0.934 5(6)	0.418 7(6)	C(201)	0.248(1)	0.299 1(6)	0.028 2(6)
C(64)	0.322(1)	0.921 8(6)	0.306 6(6)	C(202)	0.242 5(9)	0.272 8(5)	0.078 3(6)
Ni(5)	0	0	0.5	C(203)	0.199(1)	0.206 0(6)	0.049 5(6)
S(15)	0.099 0(3)	-0.052 8(2)	0.546 2(2)	C(204)	0.199(1)	0.176 0(6)	0.097 7(7)
S(25)	-0.039 8(3)	0.056 9(2)	0.581 2(2)	C(205)	0.388(1)	0.382 8(6)	0.097 0(6)
S(35)	0.162 7(3)	-0.041 1(2)	0.678 0(2)	C(206)	0.474(1)	0.349 4(6)	0.073 6(6)
S(45)	0.030 9(3)	0.059 1(2)	0.709 9(2)	C(207)	0.571(1)	0.360 0(6)	0.126 2(7)
S(55)	0.157 5(3)	0.016 6(2)	0.805 8(2)	C(208)	0.662(1)	0.329 8(6)	0.102 8(7)
C(15)	0.091(1)	-0.018 2(6)	0.619 6(6)	C(209)	0.208(1)	0.407 8(6)	0.081 5(6)
C(25)	0.030(1)	0.029 1(6)	0.633 6(6)	C(210)	0.100(1)	0.406 6(6)	0.043 0(6)
C(35)	0.120(1)	0.010 7(6)	0.733 8(6)	C(211)	0.036(1)	0.451 0(6)	0.081 1(6)
Ni(6)	0.101 0(1)	0.139 97(9)	0.429 84(9)	C(212)	-0.072(1)	0.448 6(7)	0.045 5(7)
S(16)	0.199 9(3)	0.084 7(2)	0.472 6(2)	C(213)	0.293(1)	0.384 5(5)	-0.006 2(6)

Table 1 (continued)

Atom*	X/a	Y/b	Z/c	Atom*	X/a	Y/b	Z/c
S(26)	0.067 3(3)	0.195 6(2)	0.512 6(2)	C(214)	0.320 3(9)	0.452 4(5)	0.006 0(6)
S(36)	0.267 7(3)	0.091 4(2)	0.602 3(2)	C(215)	0.337(1)	0.461 6(6)	-0.051 7(6)
S(46)	0.145 0(3)	0.195 4(2)	0.640 2(2)	C(216)	0.364(1)	0.530 6(6)	-0.042 4(7)
S(56)	0.272 2(3)	0.146 5(2)	0.731 5(2)	C(11)s	0.020(1)	0.679 2(7)	0.811 0(7)
S(66)	0.135 5(3)	0.083 8(2)	0.347 2(2)	C(12)s	0.026(1)	0.698 1(6)	0.876 1(7)
S(76)	0.003 8(3)	0.196 1(2)	0.387 0(2)	N(1)s	0.030(1)	0.713 2(6)	0.926 3(6)
S(86)	0.067 5(3)	0.089 0(2)	0.220 5(2)	C(21)s	0.066(1)	0.213 5(7)	0.812 6(7)
S(96)	-0.060 6(3)	0.190 5(2)	0.257 2(2)	C(22)s	0.038(2)	0.200 1(9)	0.859(1)
S(106)	-0.052 8(3)	0.140 7(2)	0.129 7(2)	N(2)s	0.018(1)	0.195 6(8)	0.903 7(8)

* s = Solvent.

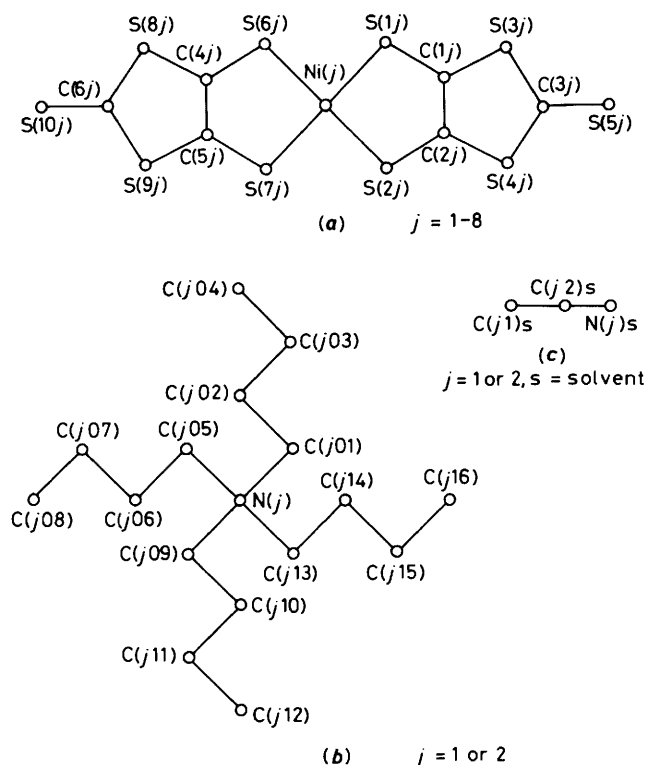


Figure 1. Labelling of non-hydrogen atoms in (a) the $\text{Ni}(\text{dmit})_2$ species, (b) the $[\text{NBu}_4]^+$ ions, and (c) the CH_3CN molecules. The digit j is used to number the crystallographically independent entities. For $[\text{Ni}(\text{dmit})_2]$ the digit j is not used

$Z = 2$, $D_c = 1.82 \text{ g cm}^{-3}$, $F(000) = 3780$, $\mu(\text{Mo-K}\alpha) = 19.4 \text{ cm}^{-1}$; at $T = 293 \text{ K}$, $a = 13.604(2)$, $b = 22.965(3)$, $c = 24.270(4) \text{ \AA}$, $\alpha = 108.16(1)$, $\beta = 103.09(1)$, $\gamma = 89.67(1)^\circ$, $U = 7000 \text{ \AA}^3$, $D_m = 1.75$, $D_c = 1.77 \text{ g cm}^{-3}$.²³

The preliminary room-temperature study²³ indicated that the determination of accurate structural parameters requires reduced thermal motion. A crystal ($0.3 \times 0.2 \times 0.1 \text{ mm}$) mounted on a CAD4 Enraf-Nonius automatic diffractometer was cooled to 118 K by a cold nitrogen gas stream produced by a locally constructed device. Accurate unit-cell parameters were obtained from least-squares calculations based on the setting angles of 25 reflections. Intensity data were collected in the $\omega-2\theta$ scan mode up to a maximum 2θ angle of 44° ($\text{Mo-K}\alpha$ radiation, $\lambda = 0.71069 \text{ \AA}$). Using the variable scan-speed technique, $17557 \pm h \pm k \pm l$ reflections were scanned of which 9858 were considered too weak to be measured. The final data set comprised 7170 independent reflections having $I > 2\sigma(I)$. No correction was made for absorption owing to the small value of the linear absorption coefficient μ .

The asymmetric unit contains 160 non-hydrogen atoms; faced with the comparatively small number of observed reflections, it was decided to refine the nickel and sulphur atoms anisotropically, the nitrogen and carbon atoms being refined with isotropic thermal parameters. Despite this limitation, there remained 1025 variable parameters to be refined. To cope with this large problem the following strategy was adopted: the least-squares refinement was conducted in the block-diagonal approximation using three blocks; the first two (432 variables each) each contained one half of the $\text{Ni}(\text{dmit})_2$ entities, and the third (160 variables) contained the $[\text{NBu}_4]^+$ cations and the solvent molecules. Atomic co-ordinates from the room-temperature study were used as starting parameters and the space group $P\bar{1}$ was assumed. All the hydrogen atoms except those of the solvent molecules were located on a Fourier difference map and introduced in idealized positions ($\text{C-H } 0.95 \text{ \AA}$, $\text{H-C-H } 109.5^\circ$) with a somewhat arbitrary thermal parameter $U = 0.05 \text{ \AA}^2$. In the final steps of the refinement the third block was kept as a fixed contribution to the calculated structure factors, and the first two blocks only were refined. The function minimized was $\sum w(|F_o| - |F_c|)^2$ where $|F_o|$ and $|F_c|$ are the scaled observed and calculated structure-factor amplitudes and $w = [\sigma(F_o)]^{-2}$. This procedure converged to $R = 0.038$ and $R' = 0.026$ where $R = \Sigma(|F_o| - |F_c|)/\Sigma|F_o|$ and $R' = [\Sigma w(|F_o| - |F_c|)^2/\Sigma w F_o^2]^{1/2}$.

The main programs used are listed in ref. 32. The atomic scattering factors were taken from ref. 33, the anomalous scattering correction being taken into account for all non-hydrogen atoms.

Non-hydrogen atom co-ordinates are given in Table 1; the atoms are labelled according to Figure 1. The bond lengths in $\text{Ni}(\text{dmit})_2$ are listed in Table 2.

(b) For $[\text{Ni}(\text{dmit})_2]$. Crystal data. $\text{C}_6\text{NiS}_{10}$, $M = 902.7$, monoclinic, space group $P2_1/a$, $a = 17.108(9)$, $b = 5.302(4)$, $c = 7.720(4) \text{ \AA}$, $\beta = 77.09(4)^\circ$, $U = 682.5 \text{ \AA}^3$, $Z = 2$, $D_c = 2.20 \text{ g cm}^{-3}$, $F(000) = 448$, $\mu(\text{Mo-K}\alpha) = 28.4 \text{ cm}^{-1}$, $T = 293 \text{ K}$.

A crystal ($0.2 \times 0.1 \times 0.005 \text{ mm}$) was mounted on a Nicolet P3F automatic diffractometer. Accurate unit-cell parameters were derived from a least-squares refinement based on the setting angles of 25 reflections. Intensity data were collected in the $\omega-2\theta$ scan mode using the variable scan-speed technique, in the range $3 < 2\theta < 45^\circ$ using $\text{Mo-K}\alpha$ radiation. 1865 $hk \pm l$ reflections were measured; 772 independent reflections having $F > 3\sigma(F)$ were retained for structure solution and refinement. No absorption correction was applied due to the small value of the linear absorption coefficient.

The structure was solved by direct methods and refined using a blocked-diagonal least-squares procedure. The final reliability factors were $R = 0.041$ and $R' = 0.049$ for 79 variables. The function minimized and the reliability factors are defined as above. The weighting scheme employed was $w^{-1} = \sigma^2(F) + 0.00026 F^2$. The programs used were part of the standard software of the diffractometer. The atomic scattering factors and the anomalous dispersion corrections were taken from ref. 33.

Table 2. Bond lengths (Å) with estimated standard deviations in parentheses in the eight crystallographically independent Ni(dmit)₂ units of [NBu₄]_{0.29}[Ni(dmit)₂]

	<i>j</i> = 1	2	3	4	5	6	7	8
Ni(<i>j</i>)-S(1 <i>j</i>)	2.152(4)	2.150(4)	2.158(4)	2.149(4)	2.153(4)	2.148(5)	2.156(4)	2.154(5)
Ni(<i>j</i>)-S(2 <i>j</i>)	2.161(4)	2.163(5)	2.158(4)	2.158(5)	2.162(4)	2.148(4)	2.148(4)	2.164(4)
Ni(<i>j</i>)-S(6 <i>j</i>)		2.152(5)	2.143(5)	2.162(5)		2.153(4)	2.151(4)	2.162(4)
Ni(<i>j</i>)-S(7 <i>j</i>)		2.149(4)	2.147(4)	2.144(4)		2.152(5)	2.142(5)	2.149(5)
S(1 <i>j</i>)-C(1 <i>j</i>)	1.69(2)	1.70(2)	1.69(1)	1.71(2)	1.73(1)	1.70(1)	1.69(1)	1.70(1)
S(2 <i>j</i>)-C(2 <i>j</i>)	1.72(1)	1.71(1)	1.71(1)	1.68(1)	1.69(2)	1.67(2)	1.67(1)	1.72(2)
S(3 <i>j</i>)-C(1 <i>j</i>)	1.74(1)	1.72(1)	1.72(1)	1.75(2)	1.75(1)	1.75(1)	1.73(1)	1.75(2)
S(3 <i>j</i>)-C(3 <i>j</i>)	1.79(2)	1.77(2)	1.73(1)	1.73(3)	1.69(1)	1.70(2)	1.76(1)	1.76(1)
S(4 <i>j</i>)-C(2 <i>j</i>)	1.71(2)	1.72(2)	1.75(1)	1.75(1)	1.75(1)	1.77(1)	1.74(1)	1.73(1)
S(4 <i>j</i>)-C(3 <i>j</i>)	1.71(1)	1.71(1)	1.74(1)	1.75(1)	1.75(2)	1.77(1)	1.73(1)	1.71(2)
S(5 <i>j</i>)-C(3 <i>j</i>)	1.63(2)	1.64(1)	1.64(1)	1.63(1)	1.66(2)	1.64(1)	1.63(1)	1.65(2)
S(6 <i>j</i>)-C(4 <i>j</i>)		1.69(1)	1.68(1)	1.70(1)		1.73(1)	1.70(2)	1.72(1)
S(7 <i>j</i>)-C(5 <i>j</i>)		1.70(2)	1.68(2)	1.71(2)		1.71(1)	1.70(1)	1.70(1)
S(8 <i>j</i>)-C(4 <i>j</i>)		1.73(1)	1.74(2)	1.73(1)		1.73(1)	1.72(1)	1.73(1)
S(8 <i>j</i>)-C(6 <i>j</i>)		1.72(1)	1.74(1)	1.76(1)		1.78(1)	1.74(1)	1.67(1)
S(9 <i>j</i>)-C(5 <i>j</i>)		1.75(1)	1.75(2)	1.72(1)		1.72(2)	1.71(2)	1.74(1)
S(9 <i>j</i>)-C(6 <i>j</i>)		1.75(1)	1.75(2)	1.73(2)		1.70(1)	1.72(1)	1.76(1)
S(10 <i>j</i>)-C(6 <i>j</i>)		1.65(1)	1.63(2)	1.62(1)		1.63(1)	1.66(1)	1.68(1)
C(1 <i>j</i>)-C(2 <i>j</i>)	1.41(2)	1.40(2)	1.38(2)	1.38(2)	1.35(2)	1.36(2)	1.42(2)	1.38(2)
C(4 <i>j</i>)-C(5 <i>j</i>)		1.40(2)	1.39(2)	1.40(2)		1.37(2)	1.42(2)	1.38(2)

Table 3. Fractional atomic co-ordinates of [Ni(dmit)₂] with estimated standard deviations in parentheses

Atom	<i>X/a</i>	<i>Y/b</i>	<i>Z/c</i>
Ni	0.5	-0.5	0.5
S(1)	0.4964(1)	-0.4071(3)	0.2316(2)
S(2)	0.4109(1)	-0.2240(3)	0.6116(2)
S(3)	0.3980(1)	-0.0256(3)	0.0833(2)
S(4)	0.3202(1)	0.1519(4)	0.4382(3)
S(5)	0.2841(1)	0.4033(4)	0.1204(3)
C(1)	0.4256(4)	-0.176 7(12)	0.2593(9)
C(2)	0.3883(4)	-0.092 4(12)	0.4282(9)
C(3)	0.3313(4)	0.189 1(13)	0.207 9(10)

Atom co-ordinates are listed in Table 3; the atoms are labelled according to Figure 1 (the *j* digit being omitted); bond lengths are listed in Table 4.

Results and Discussion

Formation of the [NBu₄]_{0.29}[Ni(dmit)₂] Conductive Species.—In the process of preparing the different members of the [Ni(dmit)₂]^{*n*-} electron-transfer series and studying the chemical or electrochemical pathways from the dianion to the monoanion and to the supposedly neutral species, we have observed²² that chemical oxidation with bromine of [NBu₄]-[Ni(dmit)₂] gave poorly characterized but electrically conductive powders. The surprisingly high compaction powder conductivity of this material, together with the results of elemental analysis, was indicative of a partial oxidation process (see Experimental section). However, as no single crystals could be obtained by chemical methods, we investigated the possible use of electrochemical synthesis. An indication of the possible utility of this approach was obtained from cyclic voltammetric studies of [NBu₄][Ni(dmit)₂]²⁴ which indicated a modification of the nature of the electrode during the oxidation step, arising from the build-up of a conductive oxidized species.

Using this observation, single crystals were grown on a platinum electrode by galvanostatic electrocrystallization of a solution of [NBu₄][Ni(dmit)₂] (see Experimental section). Thus, the electrochemical method has proved, in this case, to be most effective for obtaining single crystals and selecting the most conductive species. However, two kinds of crystals,

Table 4. Bond lengths (Å) in [Ni(dmit)₂] with estimated standard deviations in parentheses

Ni-S(1)	2.144(2)	Ni-S(2)	2.150(2)
S(1)-C(1)	1.699(7)	S(2)-C(2)	1.698(7)
S(3)-C(1)	1.731(7)	S(4)-C(2)	1.732(7)
S(3)-C(3)	1.742(7)	S(4)-C(3)	1.757(8)
S(5)-C(3)	1.625(8)	C(1)-C(2)	1.391(9)

different in morphology (needles and platelets), were obtained whose relative proportion varied with the conditions of the electrocrystallization. These two forms have the same composition, [NBu₄]_{0.29}[Ni(dmit)₂], but probably represent two different crystalline forms. Whereas a full crystal structure determination of the platelet form was successfully carried out, none of the crystals of the needle form, which are extremely thin (0.01 mm), was suitable for a structure determination; however, the X-ray powder patterns of hand-sorted out samples of needles and platelets are different; moreover, preliminary crystallographic investigations³⁴ indicated that the needles could be monoclinic, whereas the platelets are triclinic.

Four-probe Conductivity Measurements.—The conductivity of several crystals of both forms, measured along the needle axis for the needles and along the longest direction of the (001) face of the platelets, by a four-probe technique, was 1–10 Ω⁻¹ cm⁻¹. It is of interest that these values are not much higher than the compaction conductivity of powders. This provided a preliminary indication that the anisotropy in the conductivities along the different directions of the crystal is rather low, for it is well known that in one-dimensional systems the quotient σ_{crystal}/σ_{powder} is typically much higher.^{5,6}

Temperature-dependent measurements over the range 300–30 K show a thermally activated conductivity (Figure 2) for both crystalline forms. The curve of log σ versus 1/*T* is non-linear throughout this temperature range and the quite low activation energy gradually decreases (from ca. 0.1 to ca. 0.02 eV) when going from high to low temperatures. Moreover, this decrease in activation energy is much faster above ca. 130 K than below this temperature.

Such non-linear behaviour of log σ versus 1/*T* is not uncommon among the prior examples of conductive molecular solids and could arise from subtle structural changes occurring

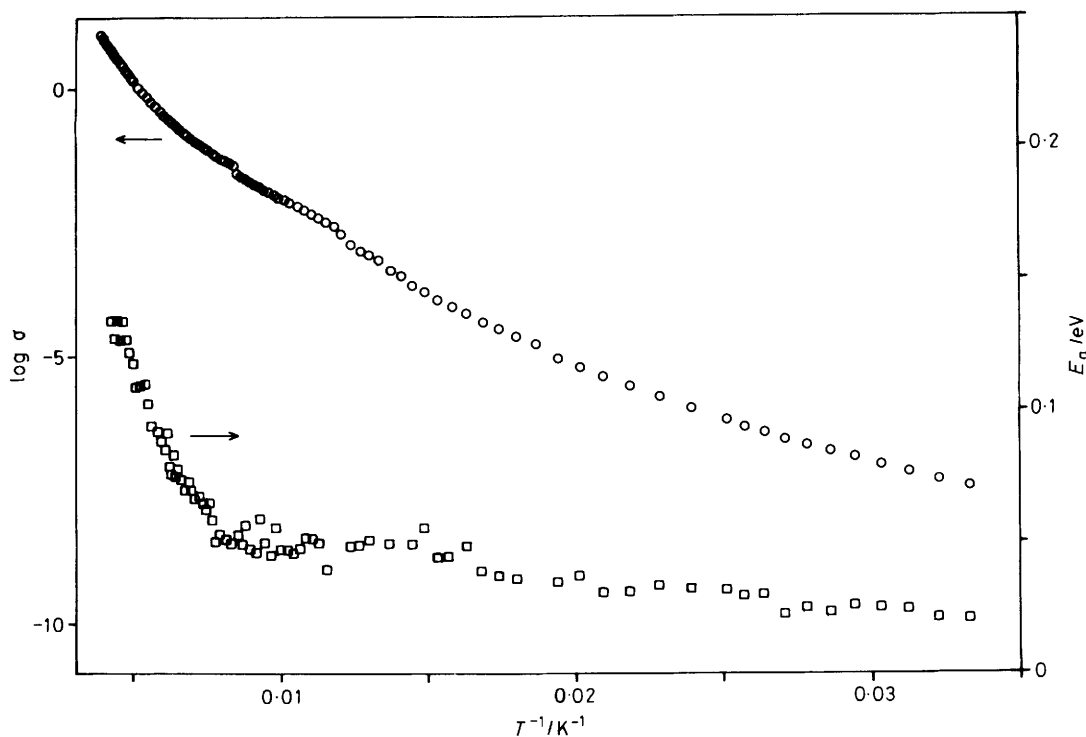


Figure 2. Four-probe conductivity measurements for $[\text{NBu}_4]_{0.29}[\text{Ni}(\text{dmit})_2]$: temperature dependence of the conductivity, $\log \sigma$ (\circ), and of the activation energy, E_a (\square)

on cooling or from changes in the carrier concentration associated with the electronic band structure of the solid. In any case it is clear that this system, although 'highly conductive' in the context of most other molecular solids, does not exhibit metal-like electrical conductivity.

Crystal Structure of $[\text{NBu}_4]_{0.29}[\text{Ni}(\text{dmit})_2]$.—The asymmetric unit contains eight crystallographically independent $\text{Ni}(\text{dmit})_2$ entities (numbered by $j = 1-8$); two of them ($j = 1$ and 5), with the nickel atom lying on a centre of symmetry, have the multiplicity $\frac{1}{2}$; in addition there are two $[\text{NBu}_4]^+$ ions and two CH_3CN solvent molecules in general positions. The formula is thus $[\text{NBu}_4]_2[\text{Ni}(\text{dmit})_2]_7 \cdot 2\text{CH}_3\text{CN}$. Ignoring the solvent molecules, the formula can be written as $[\text{NBu}_4]_{0.29}[\text{Ni}(\text{dmit})_2]$ in order to emphasize the fractional oxidation state of the $\text{Ni}(\text{dmit})_2$ species. Within the asymmetric unit, the $\text{Ni}(\text{dmit})_2$ entities are related in pairs (numbers j and $j + 4$; Figure 3) by a transformation which can be described as a translation of the nickel atoms close to $b/2$ and a rotation of the molecular mean planes by *ca.* 34° around the $\text{S}(5j)-\text{S}(10j)$ axis; the two $[\text{NBu}_4]^+$ ions and the two CH_3CN molecules are also related in pairs by a non-crystallographic translation close to $b/2$. This fact has a tremendous influence on the distribution of the intensities over the reciprocal space: the hkl reflections with $k = 2n + 1$ are considerably weakened and this explains the small proportion of measured reflections (*ca.* 44% of those surveyed).

The structure can be described as consisting of thick layers of $\text{Ni}(\text{dmit})_2$ entities parallel to (001) and separated by sheets of $[\text{NBu}_4]^+$ cations and CH_3CN molecules (Figure 4). Within a layer the $\text{Ni}(\text{dmit})_2$ species are arranged in stacks along the [110] direction (Figures 3 and 5). Two adjacent stacks are related by the transformation described above. A stack consists of quasi-parallel quasi-planar $\text{Ni}(\text{dmit})_2$ entities (Table 5) arranged in alternating centrosymmetric triads and tetrads (Figures 3 and 5). The axes of the triads and tetrads in a stack are parallel but make an angle of about 21° with the overall

stacking direction [110]. This results in the two types of overlap displayed in Figure 6. The mean distances between the $\text{Ni}(\text{dmit})_2$ least-squares planes are indicated in Figure 5 (from 3.48 to 3.57 Å); these values are typical of systems with strong intermolecular π -orbital interactions: as a comparison the regular stacking distance in the related low-temperature metallic conductor $[\text{tff}][\text{Ni}(\text{dmit})_2]_2$ is 3.55 Å.¹⁷ It should be noted here that the non-regular stacking (in distances as well as in geometry) may be responsible for the 'non-metallic' conducting behaviour of the material.

In addition to strong π interactions evidenced by the short intrastack distances, there is an extensive interleaving of the $\text{Ni}(\text{dmit})_2$ entities involving close sulphur-sulphur intermolecular contacts. The $\text{S} \cdots \text{S}$ van der Waals distance at room temperature is 3.66 Å and is likely to be less at 118 K. Intermolecular $\text{S} \cdots \text{S}$ distances less than 3.6 Å are listed in Table 6. These interactions are of two kinds. The first one (intrastack) involves partially overlapping molecules and develops in the stacking direction; these interactions are marked with an asterisk in Table 6. The second one (interstack), of a quite different type, occurs in strips roughly perpendicular to the stacking axis. The interstack $\text{S} \cdots \text{S}$ interactions are more frequent than the intrastack $\text{S} \cdots \text{S}$ interactions.

Given the π interactions along the stacks on the one hand and the interstack $\text{S} \cdots \text{S}$ interactions on the other, it is clear that the structural arrangement of $[\text{NBu}_4]_{0.29}[\text{Ni}(\text{dmit})_2]$ cannot be viewed as a classical one-dimensional system but is much more nearly two-dimensional.

Anisotropy in the Conductivities and Temperature Dependence of the Cell Parameters of $[\text{NBu}_4]_{0.29}[\text{Ni}(\text{dmit})_2]$.—The two-dimensional nature of the structure of this compound should be reflected in the anisotropy in the conductivities measured by the Montgomery method: indeed, at room temperature, the quotient of the values of the conductivities along the b and a axes, σ_b/σ_a , is about 1. This confirms that both the intermolecular interactions along the stacking direction and perpen-

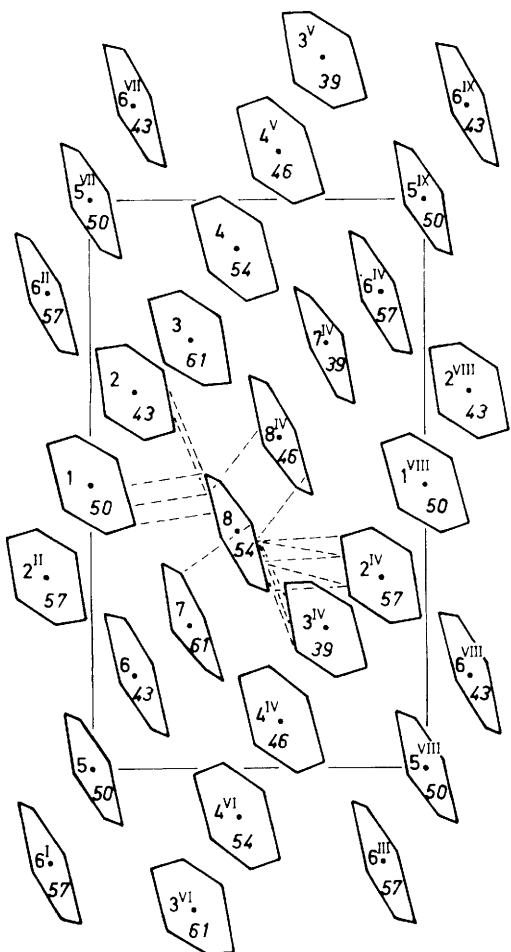


Figure 3. Orthogonal projection of a layer of Ni(dmit)_2 units of $[\text{NBu}_4]_{0.29}[\text{Ni(dmit)}_2]$ onto the (001) plane. For the sake of clarity each Ni(dmit)_2 is represented by its contour $S(5j)S(3j)S(8j)S(10j)S(9j)S(4j)$. The number j of each unit is indicated together with the z co-ordinate ($\times 100$) of the central nickel atom in italics. Roman exponents refer to the following transformations: I $-x, -y, 1-z$; II $-x, 1-y, 1-z$; III $1-x, -y, 1-z$; IV $1-x, 1-y, 1-z$; V $1-x, 2-y, 1-z$; VI $x, y-1, z$; VII $x, 1+y, z$; VIII $1+x, y, z$; IX $1+x, 1+y, z$

pendicular to this direction within the Ni(dmit)_2 strips are important in determining the pathways of electronic conductivity.

We have also carried out the Montgomery measurements as a function of temperature. The conductivities along the a and b axes follow the same general behaviour as the four-probe results, that is a non-linear variation of $\log \sigma$ versus $1/T$ with decreasing activation energy; however, σ_b/σ_a slightly increases with decreasing temperature (Figure 7) from ca. 1.1 at 250 K to ca. 1.4 at 120 K.

The contraction of the unit cell with decreasing temperature could be one explanation of the decrease in the activation energy, and the temperature-dependent variation of σ_b/σ_a could likewise be related to anisotropic temperature-dependent changes in the cell parameters. The observed decrease in a and b with decreasing temperature shown in Figure 8 is consistent with the parallel decrease of the activation energies along both the a and b axes. However, the small variation of the anisotropy in the conductivities shown in Figure 7 is not reflected in a clear similar variation of b/a which remains nearly constant (1.688 at 250 K and 1.698 at 120 K).

It is likely, therefore, that electronic effects are more important than structural changes in determining the observed temperature dependence of the conductivity.

Finally, the much lower conductivity along the third crystallographic axis c (estimated at ca. $10^{-3} \Omega^{-1} \text{cm}^{-1}$ by a two-probe technique) is consistent with the existence of a barrier formed by the layers of $[\text{NBu}_4]^+$ cations parallel to (001).

Crystal Structure of $[\text{Ni(dmit)}_2]$.—This last member of the $[\text{Ni(dmit)}_2]^n$ series was unexpectedly obtained by action of $[\text{tff}]_3[\text{BF}_4]_2$, a weak oxidizing agent [$E^\circ(\text{tff}^+ - \text{tff}^0) = 0.33 \text{ V}$ versus saturated calomel electrode (s.c.e.)], whereas bromine oxidation [$E^\circ(\text{Br}_2 - \text{Br}^-) = 0.82 \text{ V}$ versus s.c.e.] gave partially oxidized species.

The Ni(dmit)_2 molecules are centrosymmetric and close to planarity [deviations of atoms from their least-squares plane: Ni, 0; S(1), ∓ 0.001 ; S(2), ∓ 0.026 ; S(3), ∓ 0.046 ; S(4), ∓ 0.021 ; S(5), ± 0.079 ; C(1), ∓ 0.047 ; C(2), ∓ 0.039 ; C(3), $\pm 0.007 \text{ \AA}$]. These molecules stack regularly along the [010] direction, the angle of this direction with the normal to the molecular mean plane being 48° (Figure 9). Within a stack the nickel–nickel spacing is given by the b parameter (5.302 \AA) and the plane-to-plane distance is 3.562 \AA . The molecular mean planes of

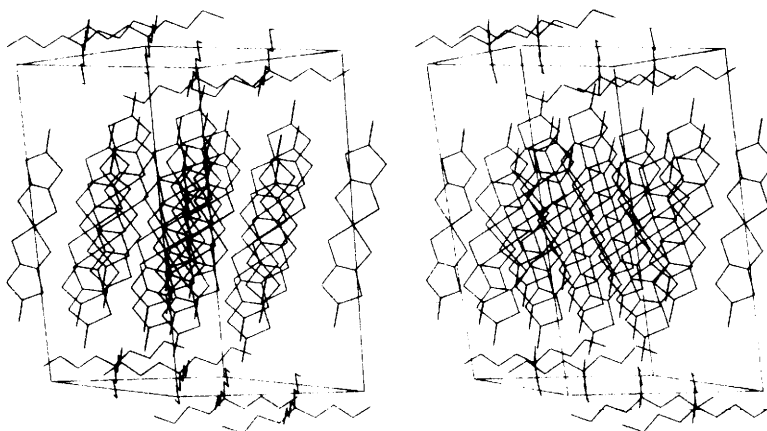


Figure 4. Stereoscopic drawing of the unit cell of $[\text{NBu}_4]_{0.29}[\text{Ni(dmit)}_2]$ viewed along a direction tilted by 10° with respect to the [110] axis. Hydrogen atoms and solvent molecules omitted

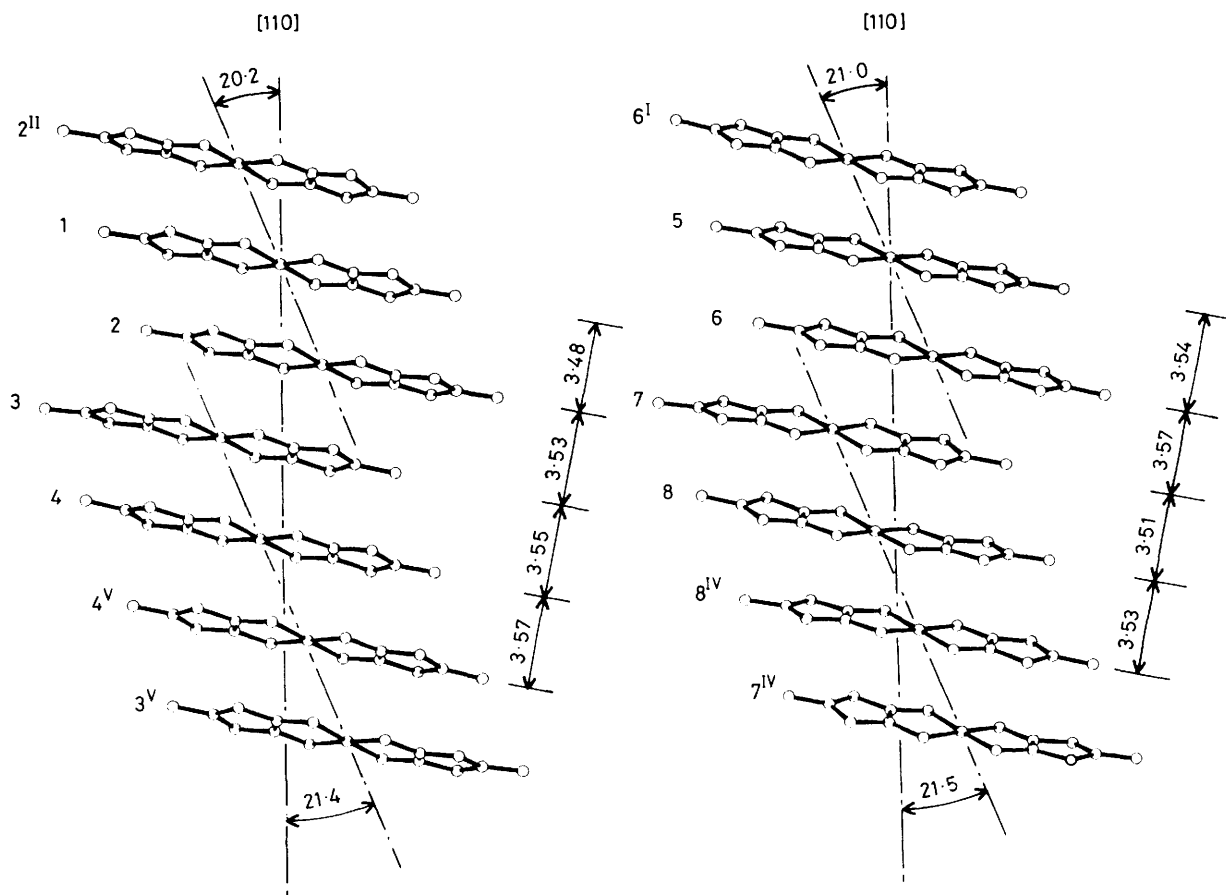


Figure 5. Stacking of the planar $\text{Ni}(\text{dmit})_2$ entities of $[\text{NBu}_4]_{0.29}[\text{Ni}(\text{dmit})_2]$ along the $[110]$ direction. Projection onto a plane containing the $[110]$ axis and the $\text{S}(5j)\text{--S}(10j)$ molecular axis. The figure emphasizes the alternation of triads and tetrad tilted by about 21° with respect to the overall stacking direction. Arabic numbers indicate the number j of each $\text{Ni}(\text{dmit})_2$. Roman exponents refer to the transformations listed in Figure 3

Table 5. Deviations (\AA) of atoms from their least-squares plane for the eight crystallographically independent $\text{Ni}(\text{dmit})_2$ units in $[\text{NBu}_4]_{0.29}[\text{Ni}(\text{dmit})_2]$ and dihedral angles ($^\circ$) between these least-squares planes

Atom	$j = 1$	2	3	4	5	6	7	8
$\text{Ni}(j)$	0	-0.018	0.016	-0.013	0	0.052	0.058	-0.038
$\text{S}(1j)$	± 0.038	-0.025	0.075	0.011	± 0.053	0.070	0.058	0.048
$\text{S}(2j)$	± 0.040	0.063	0.030	0.013	± 0.029	0.064	0.097	-0.034
$\text{S}(3j)$	± 0.017	-0.029	0.126	0.027	± 0.002	0.006	-0.092	0.051
$\text{S}(4j)$	± 0.011	0.078	-0.047	-0.055	± 0.030	-0.014	0.125	-0.001
$\text{S}(5j)$	∓ 0.056	-0.025	-0.184	0.051	∓ 0.060	-0.105	-0.191	0.047
$\text{S}(6j)$		-0.030	-0.065	-0.060		0.040	0.081	-0.106
$\text{S}(7j)$		-0.057	0.031	-0.020		0.004	-0.043	-0.055
$\text{S}(8j)$		0.065	-0.078	-0.013		-0.048	0.043	-0.042
$\text{S}(9j)$		-0.090	0.034	0.019		0.016	-0.089	0.031
$\text{S}(10j)$		0.075	-0.007	0.032		-0.065	-0.054	0.141
$\text{C}(1j)$	± 0.033	-0.009	0.109	-0.011	± 0.045	0.023	0.019	0.003
$\text{C}(2j)$	± 0.043	0.025	0.058	-0.024	± 0.038	0.026	0.101	-0.019
$\text{C}(3j)$	∓ 0.013	-0.015	-0.032	0.019	∓ 0.016	-0.041	-0.043	0.021
$\text{C}(4j)$		0.003	-0.065	-0.007		-0.004	0.017	-0.061
$\text{C}(5j)$		-0.066	-0.007	0.003		-0.009	-0.035	-0.024
$\text{C}(6j)$		0.023	0.006	0.027		-0.014	-0.051	0.036
Dihedral angles	$\left\{ \begin{array}{l} 1\text{--}5, 35.2; 2\text{--}6, 34.3; 3\text{--}7, 34.4; 4\text{--}8, 33.5; 1\text{--}2, 2.2; 1\text{--}3, 3.5; 1\text{--}4, 3.1; 2\text{--}3, 1.4; 2\text{--}4, 1.2; 3\text{--}4, 0.9; 5\text{--}6, 1.4; 5\text{--}7, 2.7; 5\text{--}8, 1.3; \\ 6\text{--}7, 1.7; 6\text{--}8, 0.9; 7\text{--}8, 1.5 \end{array} \right.$							

molecules belonging to adjacent stacks are roughly perpendicular in such a manner that this compound shows a herring bone-like structure.

As observed above in the related mixed-valence compound, there is also, in the structure of $[\text{Ni}(\text{dmit})_2]$, an interleaving of

the molecular entities involving short sulphur-sulphur distances: as shown in Figures 9 and 10, there is in this case just one such short intermolecular $\text{S}\cdots\text{S}$ contact within a stack, but there are several between molecules of adjacent stacks.

It is interesting that $[\text{Ni}(\text{dmit})_2]$ meets most of the required

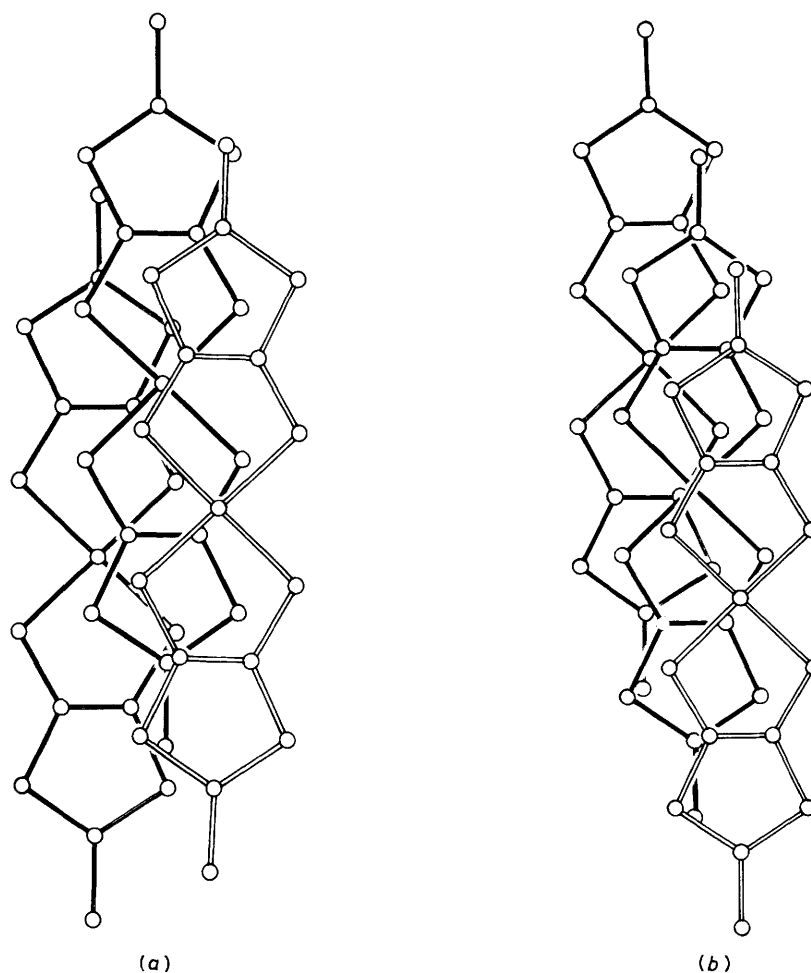


Figure 6. Overlap of the Ni(dmit)₂ species of [NBu₄]_{0.29}[Ni(dmit)₂] within a stack. The central (black) molecule may refer to; (a) *j* = 2, 3, 6, or 7; (b) *j* = 1, 4, 5, or 8

Table 6. The S...S distances (Å) less than 3.6 Å (estimated standard deviation 0.006 Å) in [NBu₄]_{0.29}[Ni(dmit)₂]. Roman exponents refer to the transformations listed in the caption of Figure 3. Intrastack interactions are marked with an asterisk

S(11)...S(78)	3.453	S(63)...S(67 ^{IV})	3.476
S(11)...S(77)	3.514	S(63)...S(68 ^{IV})	3.535
S(21)...S(98 ^{II})	3.453	S(73)...S(76 ^{II})	3.442
S(31)...S(28)	3.532	S(73)...S(15 ^{VII})	3.545
S(31)...S(52)*	3.577	S(83)...S(17 ^{IV})	3.501
S(31)...S(27)	3.583	S(83)...S(18 ^{IV})	3.523
S(12)...S(18 ^{IV})	3.522	S(93)...S(26 ^{II})	3.531
S(12)...S(78)	3.545	S(93)...S(25 ^{II})	3.596
S(12)...S(68 ^{IV})	3.570	S(14)...S(87 ^{IV})	3.520
S(22)...S(97 ^{II})	3.509	S(14)...S(16 ^{IV})	3.540
S(32)...S(68 ^{IV})	3.587	S(24)...S(35 ^{VII})	3.549
S(42)...S(76 ^{II})	3.547	S(24)...S(36 ^{VII})	3.580
S(62)...S(38 ^{IV})	3.531	S(64)...S(67 ^{IV})	3.491
S(62)...S(98)	3.559	S(64)...S(36 ^{IV})	3.525
S(62)...S(18 ^{IV})	3.592	S(74)...S(15 ^{VII})	3.463
S(72)...S(77 ^{II})	3.501	S(74)...S(16 ^{VII})	3.540
S(72)...S(27 ^{II})	3.574	S(84)...S(17 ^{IV})	3.595
S(92)...S(27 ^{II})	3.594	S(94)...S(25 ^{II})	3.419
S(13)...S(87 ^{IV})	3.543	S(25)...S(16 ^{IV})	3.585
S(13)...S(88 ^{IV})	3.591	S(107)...S(88)*	3.539
S(23)...S(96 ^{II})	3.478	S(68)...S(78)*	3.584
S(33)...S(54)*	3.578		

Table 7. Mean bond length (*D* in Å) and i.r. bands¹⁸ (cm⁻¹) in the [NBu₄]_{*n*}[Ni(dmit)₂] series with least-squares standard deviations in parentheses. Numbers in square brackets indicate the number of independent determinations

Bond*	<i>n</i> = 2	1	0.29	0
<i>a</i> { <i>D</i>	2.216(6) [2]	2.156(3) [4]	2.153(4) [28]	2.147(2) [2]
	<i>v</i>	311, 472	317, 498	328, 485
<i>b</i> { <i>D</i>	1.75(1) [2]	1.73(1) [4]	1.70(2) [28]	1.699(7) [2]
	<i>v</i>	885, 917	902	890
<i>c</i> { <i>D</i>	1.72(2) [2]	1.74(1) [4]	1.74(2) [28]	1.731(7) [2]
	<i>v</i>	885, 917	902	890
<i>d</i> { <i>D</i>	1.74(2) [2]	1.74(1) [4]	1.74(2) [28]	1.749(7) [2]
	<i>v</i>	885, 917	902	898
<i>e</i> { <i>D</i>	1.68(1) [1]	1.63(1) [2]	1.64(2) [14]	1.625(8) [1]
	<i>v</i>	1 034, 1 065	1 030, 1 060	1 064, 1 088
<i>f</i> { <i>D</i>	1.39(2) [1]	1.35(1) [2]	1.39(2) [14]	1.391(9) [1]
	<i>v</i>	1 440	1 353	1 260

* Designated according to Figure 11.

structural criteria^{6,35} for obtaining highly conducting systems, *i.e.* close regular stacking and short intermolecular contacts, but not the most important electronic criterion, *i.e.* the presence of a fractional oxidation state, and this clearly accounts for the lower conductivity of this material ($3.5 \times 10^{-3} \Omega^{-1} \text{cm}^{-1}$) at room temperature.

Structural Comparisons within the $[\text{Ni}(\text{dmit})_2]^{n-}$ Electron-transfer Series.—The crystal structures of the two first members of this series with $n = 2$ and 1 have been previously published by Lindqvist and co-workers.^{19,20} Having the present information, reported above, on the structure of the last member with $n = 0$, one may attempt to obtain a better insight into the electronic and molecular structures of these molecules and on their variation within the series, and interpolate these results to the fractional-oxidation-state complex, $[\text{NBu}_4]_{0.29}[\text{Ni}(\text{dmit})_2]$. However, such a comparison is not easy because (i) the structures of the various compounds have not been determined with the same accuracy, and (ii) the geometrical parameters of the same molecule may vary for different crystallographic sites, so that the values averaged over an idealized molecular geometry (*mmm* symmetry) have to be considered.

In this respect, we shall consider first the bond lengths of the $\text{Ni}(\text{dmit})_2$ species in $[\text{NBu}_4]_{0.29}[\text{Ni}(\text{dmit})_2]$. The eight crystallographically independent species lead to 14 or 28 independent determinations of the length of each chemically equivalent bond, and it is convenient to present Table 2 in the form of an histogram (Figure 11). This Figure emphasizes the dispersion of the results and shows that the standard deviation of the distribution is much larger than the calculated least-squares standard deviation. Several effects may combine to produce such a dispersion: (a) an artefact due to the

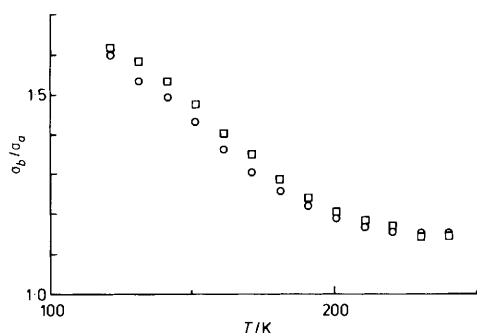


Figure 7. Anisotropy in the conductivities (σ_b/σ_a) of $[\text{NBu}_4]_{0.29}[\text{Ni}(\text{dmit})_2]$ as a function of temperature (\square , decreasing temperature; \circ , increasing temperature)

shortcomings of the model (isotropic thermal parameters, large number of unobserved reflections, etc.); (b) important distortions from the averaged geometry caused by the molecular environment, mainly the $\text{S}\cdots\text{S}$ interactions, as exemplified by the deviations from planarity listed in Table 5; and (c) the eight crystallographically independent $\text{Ni}(\text{dmit})_2$ species are not in the same electronic state.

The averaged bond lengths for the four members of the series are compared in Table 7. It is clear that the variations within the series are quite small, if not in certain cases insignificant. These bond-length variations can be tentatively rationalized in terms of a model similar to the one proposed by Schrauzer³⁶ for the metal bis(dithiolene) electron-transfer series. Following this model, the successive oxidation steps when n varies from 2 to 0

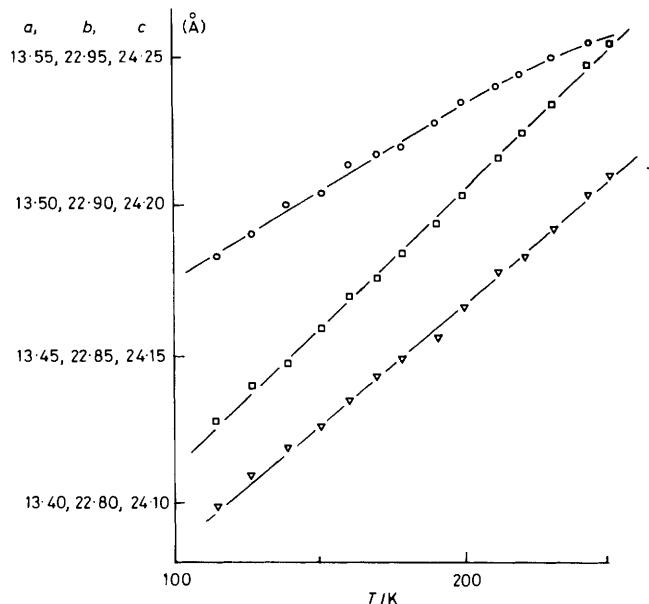


Figure 8. Temperature dependence of the unit-cell parameters a (\square), b (\triangle), and c (\circ) for $[\text{NBu}_4]_{0.29}[\text{Ni}(\text{dmit})_2]$

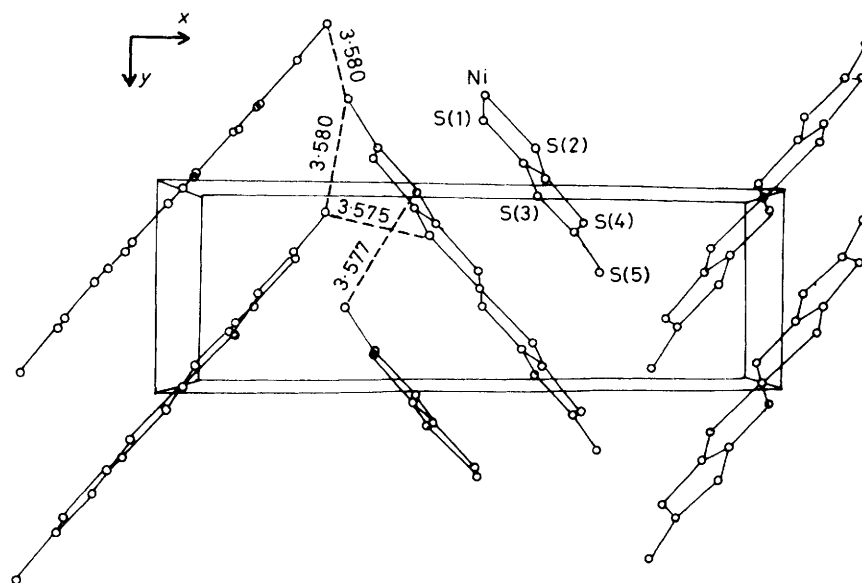


Figure 9. Perspective view along the c axis of the unit cell of $[\text{Ni}(\text{dmit})_2]$

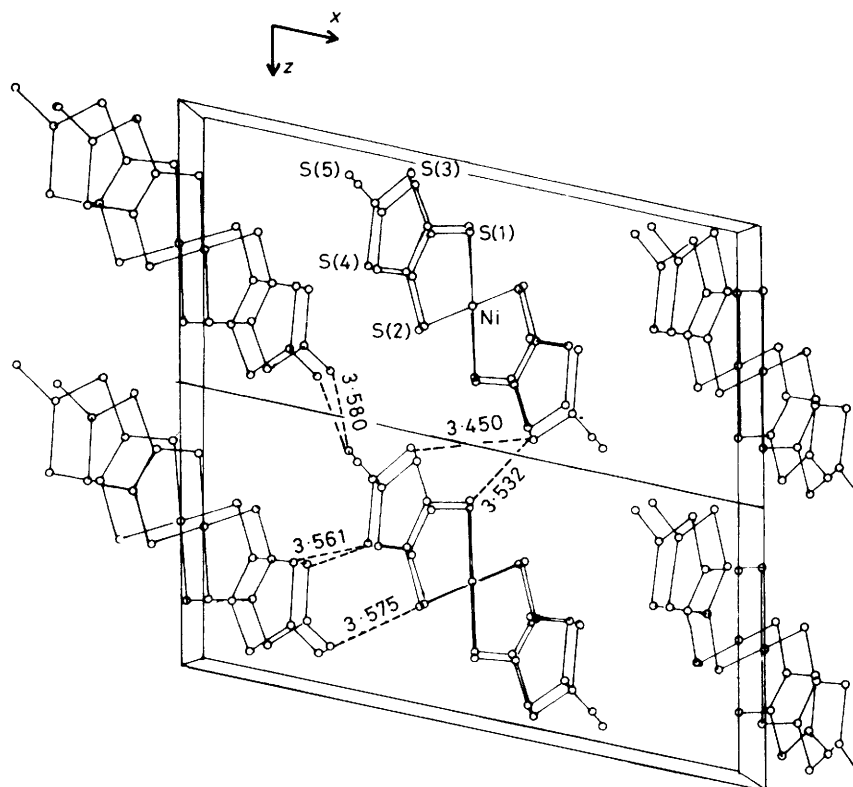


Figure 10. Perspective view along the b axis of the unit cell of $[\text{Ni}(\text{dmit})_2]$; in order to show the various $\text{S} \cdots \text{S}$ contacts, two adjacent unit cells are represented

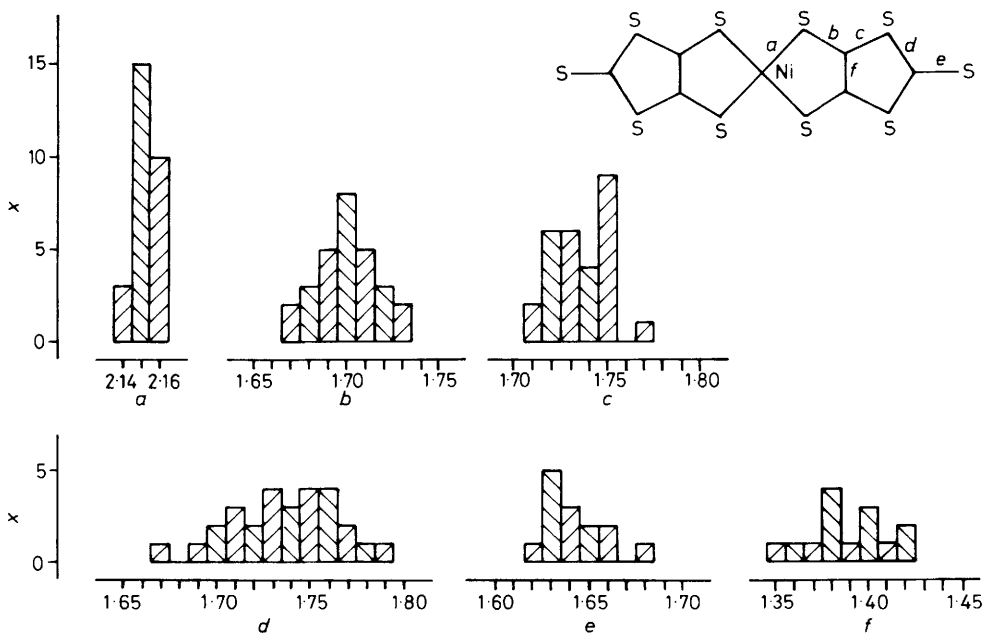


Figure 11. Histogram of the bond-length (\AA) distribution in $[\text{NBu}_4]_{0.29}[\text{Ni}(\text{dmit})_2]$ assuming an averaged mmm molecular symmetry; x is the number of independent determinations of a given bond length

should result in an increase in the dative-bond character of the nickel-sulphur bonds and an increase in the electronic delocalization within the nickel-containing five-membered rings. Moreover, in the $[\text{Ni}(\text{dmit})_2]^{n-}$ series it is interesting to verify whether this electronic delocalization is extended to the external five-membered rings and the terminal $\text{C}=\text{S}$ bonds.

The nickel-sulphur bond length decreases when n varies from 2 to 1, which is consistent with a predicted increase in the dative-bond character. However, this bond length remains roughly constant when n decreases further to 0.29 and then to 0. The b -type $\text{S}-\text{C}$ bond length decreases, slightly but significantly, when n varies from 2 to 0, which again is in agreement with increasing

delocalization in the central rings. On the other hand, the C–C bond length (f) shows no significant variation and its value remains in the range usually observed for aromatic carbon–carbon multiple bonds. The c - and d -type S–C bond lengths also remain approximately constant within the series {note the broadness of the d bond-length distribution in the case of $[\text{NBu}_4]_{0.29}[\text{Ni}(\text{dmit})_2]$. The terminal C=S bond (e) shortens and preserves its double-bond character throughout the series. In conclusion, very precise information on the electronic content and fractional oxidation state cannot be gained from these structural observations, in contrast to the case of the donor–acceptor compounds derived from tnq studied by Flandrois and Chasseau³⁷ and the $[\text{tff}]_3[\text{BF}_4]_2$ system by Legros *et al.*³⁸

Steimecke and co-workers¹⁸ have observed a noticeable decrease in a stretching frequency which they attributed to C=C vibration (see Table 7) when going from $[\text{Ni}(\text{dmit})_2]^{2-}$ to $[\text{Ni}(\text{dmit})_2]^-$, and to the compound that they supposed to be $[\text{Ni}(\text{dmit})_2]$ (and which was probably a mixed-valence species). These authors have attributed this variation to an increasing involvement of the ligand in the redox process and it is noteworthy that such an important frequency change is not reflected in a parallel bond-length variation. More consistent is the Ni–S frequency increase which is paralleled by the observed decrease in the Ni–S bond length. There are no important changes in the C–S frequencies in agreement with the C–S bond-length variations that we have observed.

Acknowledgements

The authors are grateful to the N.A.T.O. Scientific Affairs Division for support of this work. We also thank the Motorola Co., Toulouse, for supplying mounted circuits used for the conductivity measurements.

References

- S. Yamada and R. Tsuchida, *J. Chem. Soc. Jpn.*, 1949, **70**, 44; S. Yamada, *J. Am. Chem. Soc.*, 1951, **73**, 1579.
- L. E. Godycki and R. E. Rundle, *Acta Crystallogr.*, 1953, **6**, 478; S. Yamada and R. Tsuchida, *J. Am. Chem. Soc.*, 1963, **75**, 6351.
- J. S. Miller, *J. Chem. Soc.*, 1965, 713.
- C. G. Pitt, L. K. Monteith, L. F. Ballard, J. P. Collman, J. C. Morrow, W. R. Roper, and D. Ulkii, *J. Am. Chem. Soc.*, 1966, **88**, 4286; P. S. Gomm, T. W. Thomas, and A. E. Underhill, *J. Chem. Soc. A*, 1971, 2154; C. N. R. Rao and S. N. Bhat, *Inorg. Nucl. Chem. Lett.*, 1969, **5**, 531; L. V. Interrante and F. P. Bundy, *Chem. Commun.*, 1970, 584.
- H. R. Zeller, *Adv. Solid State Phys.*, (Festkörperprobleme), 1973, **13**, 21.
- 'Molecular Metals', ed. W. E. Hatfield, NATO Conference Series, Plenum Press, New York, 1979, vol. 1, series 6; P. Delhaes, *Mol. Cryst. Liq. Cryst.*, 1983, **96**, 229.
- W. A. Little, *Phys. Rev.*, 1964, **134**, 1416; D. Davis, H. Gutfreund, and W. A. Little, *ibid.*, 1976, **138**, 4766.
- K. Bechgaard, K. Carneiro, M. Olsen, F. B. Rasmussen, and C. S. Jacobsen, *Phys. Rev. Lett.*, 1981, **46**, 852; K. Bechgaard, K. Carneiro, F. B. Rasmussen, M. Olsen, G. Rindorf, C. S. Jacobsen, H. J. Pedersen, and J. C. Scott, *J. Am. Chem. Soc.*, 1981, **103**, 2440.
- Proceedings International Conference on Low-Dimensional Conductors, Boulder, 1981, *Mol. Cryst. Liq. Cryst.*, 1982, **79**, 357; 'Proceedings Colloque International du CNRS sur la Physique et la Chimie des Métaux Synthétiques et Organiques,' Les Arcs, 1982, *J. Phys. (Paris)*, 1983, **44**, C-767.
- R. E. Peierls, 'Quantum theory of Solids,' Clarendon Press, Oxford, 1955; P. M. Chaikin, *Ann. N.Y. Acad. Sci.*, 1978, **313**, 128.
- F. Wudl, *J. Am. Chem. Soc.*, 1981, **103**, 7064.
- J. M. Williams, M. A. Beno, J. C. Sullivan, L. M. Banovetz, J. M. Braam, G. S. Blackman, C. D. Carlson, D. L. Greer, and D. M. Loesing, *J. Am. Chem. Soc.*, 1983, **105**, 643; A. Beno, G. S. Blackman, P. C. W. Leung, and J. M. Williams, *Solid State Commun.*, 1985, **48**, 39.
- G. Saito, T. Enoki, K. Toriumi, and H. Inokuchi, *Solid State Commun.*, 1982, **42**, 557; H. Kobayashi, A. Kobayashi, Y. Sasaki, G. Saito, T. Enoki, and H. Inokuchi, *J. Am. Chem. Soc.*, 1983, **105**, 297.
- Y. Sasaki, G. Saito, and H. Inokuchi, *Chem. Lett.*, 1983, **4**, 581.
- S. Kagoshima, J. P. Pouget, G. Saito, and H. Inokuchi, *Solid State Commun.*, 1983, **45**, 1001.
- S. S. P. Parkin, E. M. Engler, R. R. Schumaker, R. Lagier, V. Y. Lee, P. C. Scott, and R. L. Greene, *Phys. Rev. Lett.*, 1983, **50**, 270.
- M. Bousseau, L. Valade, M-F. Bruniquel, and P. Cassoux, *Nouv. J. Chim.*, 1984, **8**, 3.
- G. Steimecke, Ph.D. Thesis, Leipzig, 1977; G. Steimecke, H-J. Sieler, R. Kirmse, and E. Hoyer, *Phosphorus Sulfur*, 1979, **7**, 49.
- L. Sjölin, O. Lindqvist, H-J. Sieler, G. Steimecke, and E. Hoyer, *Acta Chem. Scand., Ser. A*, 1979, **33**, 445.
- O. Lindqvist, L. Andersen, H-J. Sieler, G. Steimecke, and E. Hoyer, *Acta Chem. Scand., Ser. A*, 1982, **36**, 855.
- G. C. Papavassiliou, *Mol. Cryst. Liq. Cryst.*, 1981, **86**, 159; *Z. Naturforsch., Teil B*, 1981, **36**, 1200; 1982, **37**, 825; *J. Phys. (Paris)*, 1983, **44**, C3, 1257.
- J. Ribas and P. Cassoux, *C. R. Acad. Sci. Paris, Ser. II*, 1981, **293**, 287.
- L. Valade, M. Bousseau, A. Gleizes, and P. Cassoux, *J. Chem. Soc., Chem. Commun.*, 1983, 110.
- L. Valade, P. Cassoux, A. Gleizes, and L. Interrante, *J. Phys. (Paris)*, Colloq. 1983, **44**, C3, 1183.
- K. Hartke, T. Kissel, J. Quante, and R. Matusch, *Chem. Ber.*, 1980, **113**, 1898.
- S. Wawzonek and S. M. Heilman, *J. Org. Chem.*, 1974, **39**, 511.
- G. Bontempelli, F. Magno, G. A. Mazzochin, and R. Seeber, *J. Electroanal. Chem. Interfacial Electrochem.*, 1975, **63**, 231.
- M. F. Hurley and J. Q. Chambers, *J. Org. Chem.*, 1981, **46**, 775.
- J. Clavilier, R. Faure, G. Guinet, and R. Durand, *J. Electroanal. Chem., Interfacial Electrochem.*, 1980, **107**, 205.
- G. Commenges and P. Cassoux, *Spectra 2000*, 1982, **10**, 34.
- H. C. Montgomery, *J. Appl. Phys.*, 1971, **42**, 2971.
- CAD4 CICT 10; a local program for data reduction, J. Aussoleil and J.-P. Legros, 1980; SHELX 76 and SHELXTL, computer programs for crystal structure determination, G. M. Sheldrick, 1976; NUCLS, least-squares program, R. Doedens and J. A. Ibers, 1978, based on W. R. Busing and H. A. Levy's ORFLS, 1962; ORTEP, C. K. Johnson, 1965; ORFFE, function and error program W. R. Busing, K. O. Martin, and H. A. Levy, 1964.
- 'International Tables for X-Ray Crystallography,' Kynoch Press, Birmingham, 1974, vol. 4.
- A. Gleizes, personal communication.
- J. Miller and A. Epstein, *Prog. Inorg. Chem.*, 1976, **20**, 1; J. H. Perlstein, *Angew. Chem., Int. Ed. Engl.*, 1977, **16**, 519.
- G. N. Schrauzer, *Acc. Chem. Res.*, 1969, **2**, 72.
- S. Flandrois and D. Chasseau, *Acta Crystallogr., Sect. B*, 1977, **33**, 2744.
- J.-P. Legros, M. Bousseau, L. Valade, and P. Cassoux, *Mol. Cryst. Liq. Cryst.*, 1983, **100**, 181.

Received 5th July 1984; Paper 4/1156